Construction and Building Materials 458 (2025) 139554

Contents lists available at ScienceDirect

Construction and Building Materials

journal homepage: www.elsevier.com/locate/conbuildmat

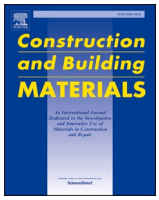

Durability of biochar-cementitious composites incorporating crystalline admixture in chloride and sulphate environments

Xuqun Lin [a], Quang Dieu Nguyen [a,*], Arnaud Castel [a], Yu Pang [a], Zhizhong Deng [a], Tianxing Shi [a], Wengui Li [b], Vivian W.Y. Tam [c]

[a] School of Civil and Environmental Engineering, University of Technology Sydney, NSW 2007, Australia
[b] Centre for Infrastructure Engineering and Safety, School of Civil and Environmental Engineering, The University of New South Wales, NSW 2052, Australia
[c] Westen Sydney University, School of Engineering, Design of Built Environments, NSW 2751, Australia

ARTICLE INFO

Keywords:
Crystalline admixtures
Biochar
Durability
Microstructure
Chloride
Sulphate
Strength reduction
SEM-EDS

ABSTRACT

This study investigated the effects of crystalline admixture (CA) and waste wood biochar (WWB) on sulphate and chloride ions penetration resistance of coastal concrete infrastructure. Three solutions (e.g. water, 5 % Na_2SO_4 solution, and 5 % NaCl solution) were prepared for cement paste specimens immersion up to 156 days. Strength developments, water adsorption, and Scanning Electron Microscopy (SEM) analysis were carried out. It was found that CA and WWB addition reduced the water adsorption and promoted a slight increase of the mechanical strength in water curing condition up to 156 days. After 28 days of Na_2SO_4 solution immersion, due a denser microstructure, CA and WWB addition led to 15.1–16.2 % and 17.9 – 20.93 % reduction in Na_2SO_4 solution adsorption respectively, while improving the mechanical properties when compared to the reference group. SEM-EDS presented the formation of ettringite in WWB's pore, densifying the biochar-cement composites. However, due to the continuous formation of ettringite and gypsum, excessive cracks were observed, increasing Na_2SO_4 solution adsorption and lowering the mechanical strength improvement for samples with CA and WWB addition. CA and WWB addition resulted in 17.16 – 18.1 % and 20.85 – 23.23 % reduction in 28-day NaCl solution adsorption respectively and reduced the 156-day NaCl solution adsorption by 15.2–15.8 % and 17.8 – 20.1 % respectively. Meanwhile, both CA and WWB led to mechanical strength improvements when compared to the control group at all ages, samples with 1 wt% CA addition had lowest strength reduction rate. Overall, the findings suggested that the presence of CA and WWB will improve the durability properties of coastal structures immersed in seawater.

1. Introduction

Cementitious composites are vulnerable in coastal areas, since aggressive ions including chlorides and sulphates can penetrate into the concrete microstructure to reduce the structure service life [1–3]. Li et al. [4] mentioned that chlorides pose significant challenges to concrete structures, by lowering the ultimate capacity due to reinforcement corrosion. Several studies [5–7] found that the presence of sulphates resulted in excessive formation of ettringite and gypsum, causing concrete strength loss and microstructural cracks. As a result, proper strategies need to be used to mitigate the access of aggressive ions into the cementitious structures in coastal areas.

Many studies [8–10] reported that using supplementary cementitious materials (SCMs) can improve the mechanical properties of the cementitious composites while improving their resistance of chloride and sulphate ingress by reducing the porosity. Li et al. [8] observed that replacing Ordinary Portland cement with 5 wt% silica fume (SF) led to lower compressive strength degradation when compare to that of the control group after 90-day sulphate attack. They also found that lower RCPT charge passed was found in samples with 5 wt% silica fume (SF) when compared to samples without SF, indicating high chloride resistance due to presence of SF. Rashad et al. [2] used 20 wt% metakaolin (MK) to replace Portland cement in FA-cement composites. They found that the addition of metakaolin led to a denser cementitious microstructure, leading to 8.8 % and 6.5 % compressive strength increase exposed to seawater and tidal zone in 9 months respectively when compared to MK-free samples. Yang et al. [11] found that incorporating fly ash could refine the pore structures of the cementitious composites,

* Corresponding author.
E-mail address: quangdieu.nguyen@uts.edu.au (Q.D. Nguyen).

https://doi.org/10.1016/j.conbuildmat.2024.139554
Received 16 September 2024; Received in revised form 20 November 2024; Accepted 10 December 2024
Available online 14 December 2024

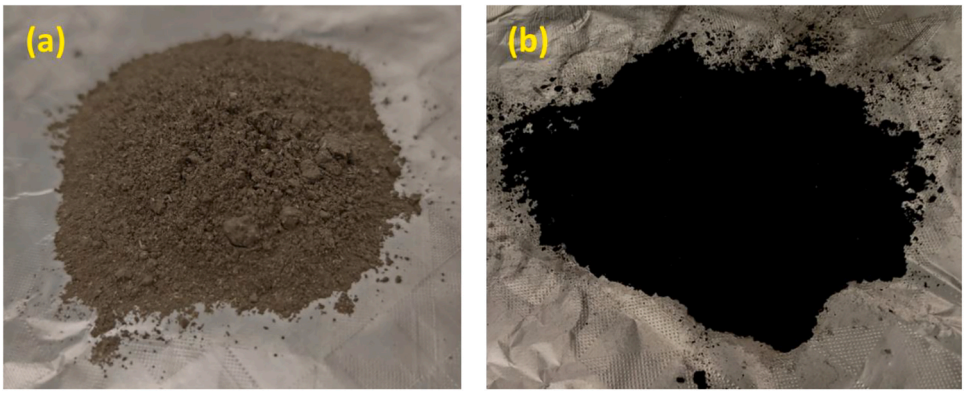

Fig. 1. Raw materials morphology: (a) CA and (b) WWB.

leading to a denser microstructure to resist aggressive ion penetration. Hu et al. [12] reported that 25 % addition of fly ash resulted in an improvement in both mechanical strength and chloride resistance. Chen et al. [13] incorporating 10–30 % barium slag promoted the chloride diffusion resistance with less porosity. Similarly, Ukpata et al. [14] concluded that in addition to pore refinement, ground granulated blast furnace slag (GGBFS) improved the chloride-binding compacity of the slag-cement composite, reducing the chloride-ion penetrations. Although those industrial by-products are efficient in replacing cement, their transportation could be contributing to a high carbon footprint and cost for many countries without such material availability.

Recently, biochar, produced by the pyrolysis of different biomass in an oxygen-free environment, has received increasing attention as an environmental-friendly SCMs to produce sustainable concrete [15–17]. Lin et al. [17] mentioned that the application of biochar in cementitious composites led to two benefits, including lowering the carbon footprint and promoting the recycling of different biomass rather than traditional treatments involving burning and landfill. In terms of mechanical properties, Javed et al. [18] observed that after adding 2 wt% bagasse biochar, the compressive strength was improved by 18 % when compared to the control group, due to relative small particle size ($< 75\mu m$) providing proper filler effect. Sirico et al. [19] found that woodchip biochar increased the load-bearing capacity of the cementitious composites, and biochar particles altered the cracking propagation path allowing to resist higher loads. Similarly, Mishra et al. [20] reported the improvement of the flexural strength of biochar-cement composites which was mainly due to the biochar particles interfering the cracks propagation. Regarding durability properties, several studies [21–23] concluded that cementitious composites with biochar addition had lower water permeability, being favourable to resist aggressive-ion penetrations. However, the investigations of potential effects of biochar addition on long-term aggressive-ion ingress are limited. In Australia, wood-related products play an important role in Australian economy [24]. Kaseasbeh & Qaralleh [25] reported that up to 40 % waste wood remained unrecycled in many countries, including Australia, UK, and USA. As a result, it is worthy analysing the feasibility of recycling waste wood as waste wood biochar to partially replace cement to design sustainable concrete with high resistance against the penetration of aggressive ions.

Another promising approach to reduce the porosity of the cementitious composites is the incorporation of crystalline admixture (CA), mainly used as permeability-reducing agent and self-healing agent [26–28]. Due to similar chemical compositions of CA compared to cement, Several studies reported that CA addition did not affect the workability [29,30] and hydration process [31,32] of the CA-cement composites. Ding et al. [33] reported that CA could induce the formation of insoluble crystals to fill in pores and cracks of cementitious materials, promoting the self-healing behaviour of mortars and concretes. Similarly, Wang et al. [34] mentioned that CA powder could react with cement hydration products, densifying the cementitious matrix and limiting the penetration of water and chlorides. Several studies [29,35,36] observed that CA addition led to better chloride penetration resistance via rapid chloride penetration test (RCPT). However, there are limited studies accessing the performance of concrete with CA addition subjected to long-term chloride and sulphate solution immersion.

This study primarily aims to investigate the effects of crystalline admixture (CA) and waste wood biochar (WWB) addition on the long-term resistance against chlorides and sulphates, targeting cementitious composites in coastal regions. Although seawater contains chloride and sulphate ions, it is important to assess how the degradation of the cementitious composites would occur in chloride and sulphate solutions separately. As a result, 5 % Na_2SO_4 and 5 % NaCl solutions were prepared, and specimens were exposed up to 156 days. This study analysed the mass change and strength degradation of cement paste specimens after 28 days, 96 days, and 156 days of immersion. Scanning electron microscopy (SEM) equipped with energy dispersive X-ray spectroscopy (EDS) was used to investigate the microstructural degradation and the chemical compositions of the products producing after the sulphate and chloride exposure. X-ray Diffraction (XRD) was used to analyse sulphate-attack products up to 156 days.

2. Materials and methodology

2.1. Raw materials

General purpose cement (GPC) traded by Boral Australia was used in this study. Crystalline admixture (CA) by PENETRON Admix® Australia was used, shown in Fig. 1a. Several studies [28,37–39] mentioned that powder-form CA contained high volume of cement (up to 80 wt%) and unknown chemicals, due to patent protection. It is evident in XRD pattens results (Fig. 2a), where CA mainly contained alite, belite, and small amount of portlandite, quartz, and calcite. Blended waste wood biochar was purchased from Green Man Char (Australia) and grounded into powder (Fig. 1b), named as WWB. Fig. 2b shows the particle size distribution of CA and WWB, analysed by laser diffraction technique, WWB size being less than 200 μm. Based on the study by Lin et al. [17], small size of WWB could benefit the void-blocking effect on the biochar-cement matrix. The majority of CA powder was less than 100 μm, with approximately 2 % of ranging between 100 and 500 μm, which could be identified as the special chemicals.

Fig. 3 presents the SEM images of CA and WWB in different magnifications. CA powders (Fig. 3a) have irregular shape, and the microstructure of WWB (Fig. 3b) is porous with randomly distributed pores. It could be observed that WWB has thick wall, significantly different to the thin wall in juliflora biochar in the study by Pawar & Panwar [40], indicating the microstructure variability of different biochar. Table 1 presents the chemical compositions determined by the XRF test of GP,

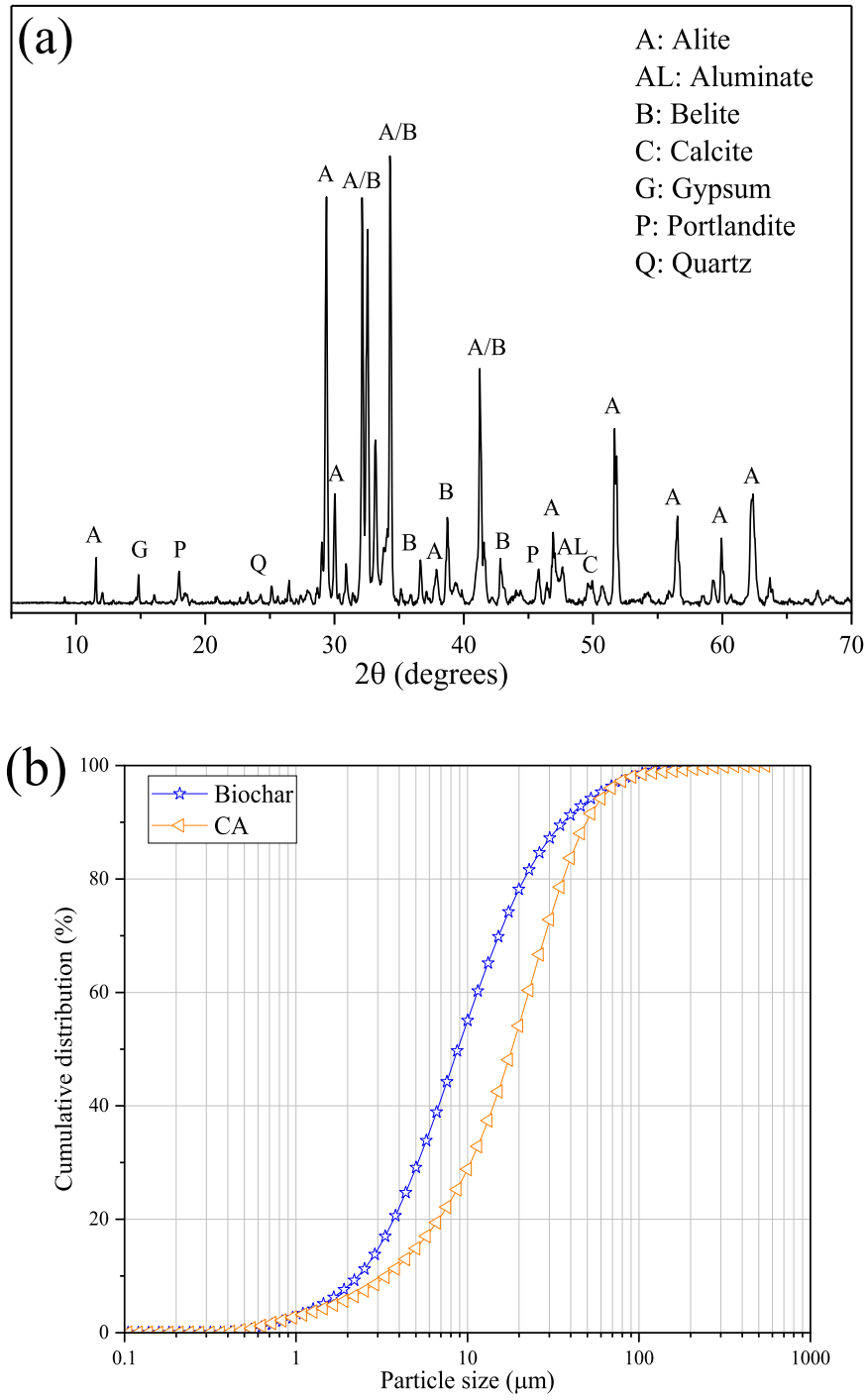

Fig. 2. (a) XRD pattens of crystalline admixture; (b) Particle size distribution analysis of biochar and crystalline admixture.

CA, and WWB. Due to the presence of special chemicals, the chemical composition of CA is slightly different to that of GPC. For CA, the percentage of Na_2O is 9.15 %, being significantly higher than that (0.25 %) of GPC. The Loss of Ignition of CA is also higher than that of GPC. According to Table 1, WWB has higher content of silica (58.20 %), which may benefit the process of pozzolanic reaction of the biochar-cement composites.

2.2. Specimen preparation

To investigate the potential effects of CA and WWB addition on the resistance against aggressive-ion ingress of the cementitious composites, six mix designs were adopted (Table 2). Water to binder ratio (w/b) of 0.35 was set for all groups. CO group had only GPC as binder material, being the reference group. For CA and CA2, 1 wt% and 2 wt% CA was added in the mix design. As a result, it could be used to compare the performance of the cementitious composites with and without CA addition. Furthermore, based on the study by Lin et al. [17], using 2–5 wt% biochar (< 200 μm) in replacing cement did not lead to reduction of the mechanical properties of the biochar-cement composites. Hence, this study adopted using 5 wt% biochar replacing cement, denoted as BC group. Superplasticizer (Sikament® Eco WR, Sika Australia) was added in the biochar-cement composites to maintain similar slump when compared to the reference group (Table 2). CB and

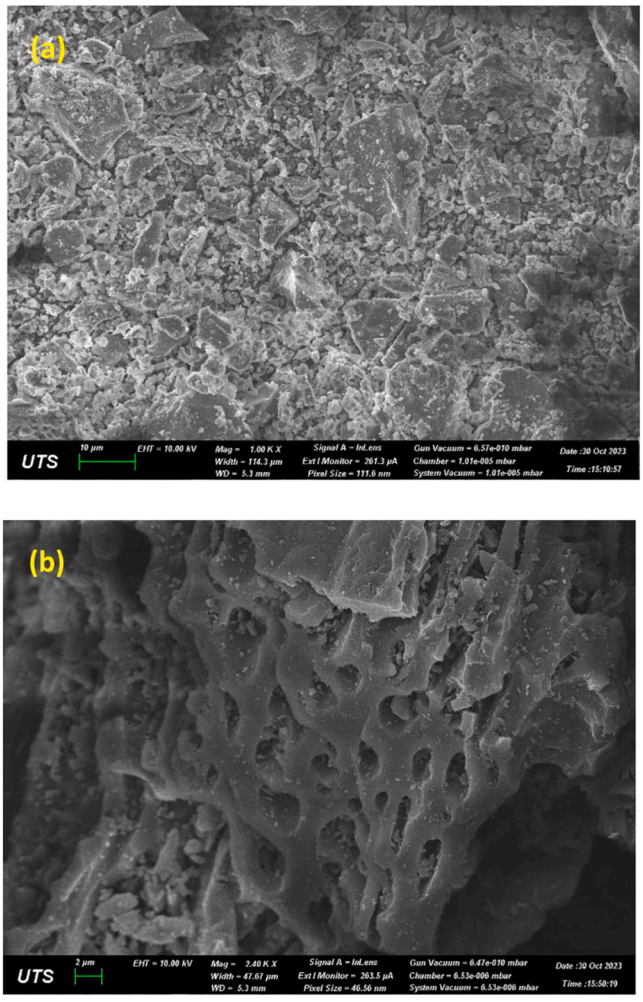

Fig. 3. Microstructural morphology: (a) CA and (b) WWB.

Table 1
Chemical compositions of raw materials.

Chemical compositions (%)	CA	GPC	WWB
SiO_2	14.15	18.94	58.20
P_2O_5	0.17	0.20	2.29
SO_3	1.83	2.49	1.35
CaO	49.24	63.73	19.73
K_2O	0.74	0.47	2.88
TiO_2	0.12	0.29	0.27
Al_2O_3	3.73	5.14	3.95
Fe_2O_3	1.76	3.00	1.67
Na_2O	9.15	0.25	5.10
MgO	3.27	1.48	3.45
V_2O_5	< 0.01	0.02	< 0.01
Cr_2O_3	0.01	0.02	0.05
Mn_3O_4	0.08	0.19	0.50
LOI	15.78	4.09	0.50

CB2 were named after adding 1 wt% and 2 wt% CA respectively. Potential effects of WWB addition on the resistance against aggressive-ion ingress could be analysed with and without CA. It should be noted that CA is primarily added into the cementitious composites, while WWB is used to partially replace cement for sustainable cementitious design purpose.

The mixing equipment was 10 L Hobart Mixer. Firstly, a low-speed mixing with 16 rpm was used for 2 mins to achieve uniform powder mixture, and ½ water was then added and mixed using the same low-speed mixing for 1 min. After that, another ½ water was mixed with medium-speed mixing with 24 rpm for 2 mins. Another 2 min low-speed mixing was conducted after shovelling the binder materials from the wall of the mixer. The fresh cementitious pastes were then poured in moulds with dimensions of 40 × 40 × 160 mm, and a 3-minute vibration was applied to all moulds to promote uniform compaction. This study aimed to investigate the performances of CA and WWB addition on the resistance against aggressive-ion ingress after 28 days, 96 days, and 156 days of exposure. Each case would be investigated using three prisms. Hence, totally nine prisms were casted for each mix design. It should be noted that all prism moulds were covered by plastic foil for 24-hour curing. After demoulding, cementitious prisms were stored in a conditioned chamber with 95 ± 5 % relative humidity and 23 ± 2 °C. According to several studies [5,7], before being exposed to sulphate and chloride solutions, the immersed samples should achieve a minimum compressive strength of 20 MPa in accordance with ASTM C1012. As a result, after demoulding, all cementitious prisms would be stored in the conditioned chamber for another three days.

Table 2
Mix design of different cementitious composites.

Design	Biochar (wt%)	CA (wt %)	Cement (wt%)	w/b	Superplasticizer (wt%)	Slump (mm)
CO	0	0	1	0.35	—	227 ± 1.3
CA	0	0.01	1	0.35	—	225 ± 2.3
CA2	0	0.02	1	0.35	—	226 ± 1.5
BC	0.05	0	0.95	0.35	0.012	224 ± 1.8
CB	0.05	0.01	0.95	0.35	0.012	224 ± 2.5
CB2	0.05	0.02	0.95	0.35	0.012	224 ± 2.1

After 3-day curing, hardened cementitious specimens were completely immersed in three different solutions in plastic containers stored in a room with temperature of 23 ± 2 °C, including water as reference solution, 5 % Na_2SO_4 solution, and 5 % NaCl solution. 5 % Na_2SO_4 and 5 % NaCl solutions were prepared using deionised water and reagent grade sodium sulphate and sodium chloride pellets. All solutions were renewed weekly over the first month of immersion, and thereafter biweekly, mitigating the potential pH increase due to OH^- leaching.

2.3. Mass measurements

The initial mass of all cementitious samples was measured by using a digital weighting device with an accuracy of ± 0.001 g before being exposed to three solutions, donated as m_i. The excessive water on the specimens' surface was wiped before taking the measurements. After that, the mass measurements were conducted once a day over the first 28 days and then performed weekly up to 156-day of exposure, donated as m_t. Change in mass was calculated based on Eq. 1. Three samples were measured for each group, and the average results were plotted for discussions.

$$\text{Change in mass}(\%) = \frac{(m_t - m_i)}{m_i} \times 100\% \quad (1)$$

It should be noted that the measurement of the time-dependent sample length changes was not carried out in this study. However, it will be carried out as a part of a future investigation assessing the self-healing behaviour of biochar-cement composites incorporating CA in sulphate and chloride environments. The potential expansion or shrinkage of the samples exposed to sulphate and chloride environments may affect the self-healing capacity of the cementitious composites. This

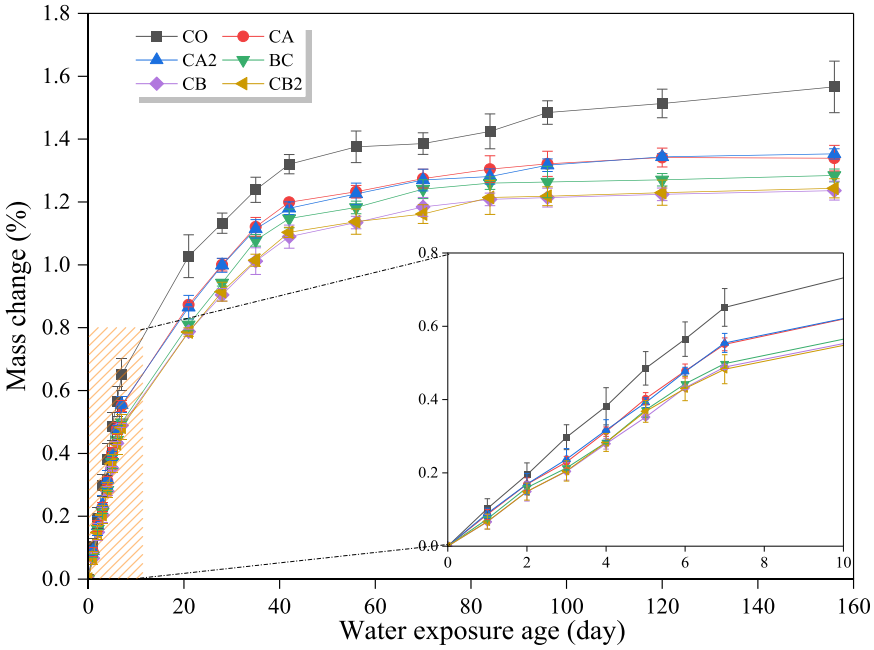

Fig. 4. Mass change of samples immersed in water.

will be investigated by combing length measurements and self-healing behaviour together to establish potential relations.

2.4. Mechanical properties degradation

The flexural strength of samples after different exposure times was investigated setting up a 3-point bending test using a AGX 50 universal testing machine as per ASTM C348–21 [41]. Based on ASTM C349–18 [42], the broken portions of samples following the bending test could be directly used in compression experiments. The compressive strength of the samples was measured using a AGX 500 universal testing machine. The final flexural strength (f_f) and compressive strength (f_c) of each type of specimens were the average value of three samples.

2.5. Microstructural analysis

The microstructural analysis was carried out using a Zeiss Supra 55VP Scanning Electron Microscopy (SEM) with energy dispersive X-ray spectroscopy (EDS). According to several studies [7,43], aggressive ions could penetrate into the cementitious matrix within the range of 1–10 mm after 1 month. Following the compression test, small pieces of samples within this depth range were selected and cast within a cylinder-shape epoxy resin followed by a polishing process. After that, polished samples were stored in a vacuum oven at 60 ℃ for 1 week and coated with 8 nm gold using Leica EM ACE600 coater. The operating voltage was 10 kV, and the working distance was set in the range of 5–8.5 mm for microstructural identifications and EDS analysis.

Small paste samples collected following the 156-day compressive strength tests were immersed in isopropanol until grinding. It should be noted that samples of each group were grinded into powder using a ring mill, dried in an oven at 60°C for 3 days. XRD analysis was conducted using a Bruker D8 Discover diffractometer (Cu Kα, λ = 1.54 Å). The measuring range was set from 5° to 70° using a sample spinner at the scanning step of 0.03°. Crystallography Open Database was utilised for mineralogy characterisation of phases after 156-day sulphate exposure.

3. Experimental results

3.1. Water exposure

The mass change as a function of the time of exposure for the six groups is depicted in Fig. 4. It could be observed that the addition of CA and WWB reduced the water adsorption over the whole exposure period when compared to the control group CO (black line). In terms of CA addition only, 1 wt% (red line) and 2 wt% CA addition (blue line) promoted 11.7 % and 11.9 % reduction in mass increment at 28-day water exposure respectively, being in a good agreement with several other studies [36,44]. Aspiotis et al. [36] reported that CA powder stimulated crystals blocking pores and limiting water access into the cementitious matrix, reducing the water permeability. It should be noted that due to the continuous water ingress, CO group had the highest mass increment at 156-day exposure. 1 wt% and 2 wt% CA addition reduced the mass increase by 14.4 % and 13.6 % respectively at 156-day exposure. Due to a denser microstructure, CA and CA2 groups had the lowest mass increase rates, achieving high resistance against water adsorption at long-term exposure. However, increasing the dosage of CA addition seemed not to further improve the water-ingress resistance, since CA and CA2 groups performed similarly.

For BC group with 5 wt% WWB replacing cement, a mass increase reduction of approximately 16.7 % and 17.9 % was observed after 28-day and 156-day of water exposure respectively. As shown in Fig. 2, approximately 80 % of WWB particles were smaller than 20 μm, providing a proper filler effect blocking the voids of the biochar-cement matrix. Furthermore, porous biochar could provide additional hydration sites improving the cement hydration and reducing the water permeation [45,46]. CB and CB2 group had the lowest water absorption with the combination of CA and WWB addition. Fig. 4 shows 21.1 % and 20.6 % reduction in mass increase at 156-day water exposure for CB and CB2 respectively. Although WWB offered improved hydration and favourable filler effect, CA addition induced additional crystalline deposits blocking voids and pores and improving the compactness of the cementitious matrix. As a result, the combination of CA and WWB promoted the best performance in mitigating water ingress.

The strength development of the different cementitious specimens cured in water for 28 days, 96 days, and 156 days are presented in Fig. 5.

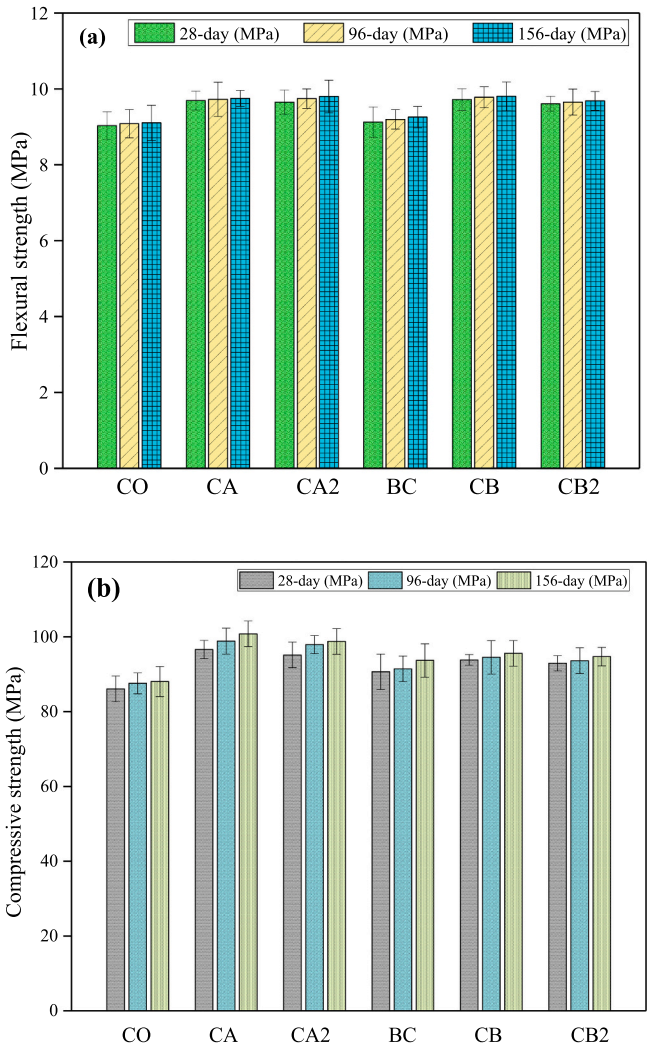

Fig. 5. Strengths development of samples cured in water: (a) Flexural strength and (b) Compressive strength.

As shown in Fig. 5a, while replacing cement by 5 wt% WWB, the flexural strength of BC group was very similar to that of the reference CO group at three exposure ages. Although WWB could promote the hydration of the cementitious composites, excessive amount of porous biochar inevitably creates weak points in the interfacial transition zone (ITZ), lowering the strength increment. Similarly, Gupta et al. [45] explained that while 1 wt% biochar promoted 10–13 % flexural strength increase compared to the control group, samples with 5 wt% biochar achieved a similar flexural strength when compared to the plain samples. They pointed out that more porous areas in the tensile plane of the biochar-cement composites with 5 wt% biochar reduced the load-bearing capacity. However, due to crystal deposit induced by CA, the flexural strengths of CA, CA2, CB, and CB2 were slightly higher than that of the CO group, being 7.3 %, 6.8 %, 6.9 %, and 6.3 % respectively. It should be noted that a higher dosage of CA did not lead to a higher flexural strength development.

For the compressive strength development, the cementitious composites with CA, WWB, or both additions performed better than the reference in Fig. (5b). While there was only 6.5 % compressive strength increment for BC group, higher strength increments were observed in samples with CA addition at 28 days, being 12.2 %, 10.5 %, 10.4 %, and 9.22 % for CA, CA2, CB, and CB2 respectively. Lin et al. [17] stated that unlike flexural strength, biochar addition could lead to an improvement of the compressive strength due to a denser microstructure. The primary

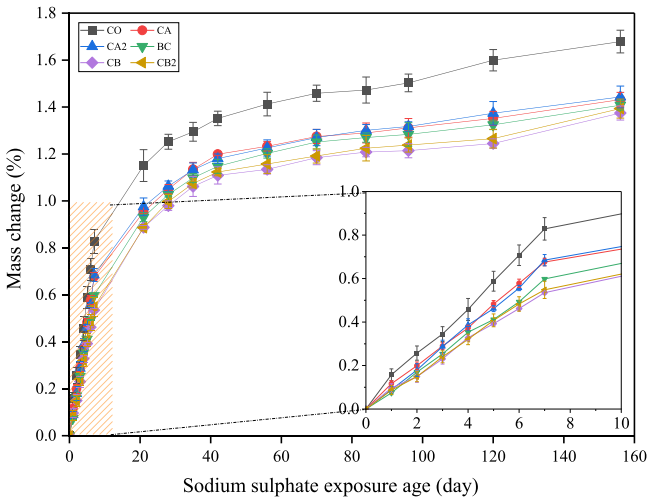

Fig. 6. Mass change of specimens in 5 % sodium sulphate immersion.

reason is that compressive forces tend to close the porous area in the cementitious matrix, while the pores at bottom sections of the specimen are opening when subjected to flexural forces [45,47].

Overall, all samples' compressive strength increased up to 156 days, and the compressive strength increase was higher than that of flexural strength. The reason is that although both CA and WWB can lead to a denser cementitious microstructure, this would not significantly change the brittle nature of the cementitious composites, limiting the increase in the flexural capacity.

3.2. *The 5 % sodium sulphate solution exposure*

As shown in Fig. 6, the mass increments of all samples exposed to the 5 % sodium sulphate solution were higher those of samples immersed in water. For the control group CO, the mass increments were 1.25 % and 1.68 % for 28-day and 156-day of Na_2SO_4 exposure respectively. Due to the continuous sulphates ingress at 28 days, numerous ettringite and gypsum were found (Fig. 7a), and SEM-EDS results (Fig. 7b) confirmed that the formation of ettringite led to unfavourable cracks in the cementitious matrix of CO samples. In terms of CA addition, the formation of crystalline deposits mitigated the access of sulphate ions into the CA-cement matrix, leading to 16.2 % and 15.1 % reduction in the mass increase when compared to CO group after 28-day of Na_2SO_4 exposure. At 156-day immersion age, specimens with CA addition only presented a mass increase reduction of 14.7 % and 14.06 % for CA and CA2 samples respectively. Due to the long-term immersion, more cracks inevitably created more accessible channels for penetration into the cementitious matrix in Fig. 8(a), leading to higher water and sulphate adsorption. Similar finding was reported by Dobrovolski et al. [48], reporting that although CA mitigated the access channel for sulphates and water, more cracks in the cementitious microstructure were formed due to the long-term immersion, increasing the water and sulphate adsorption. However, the mas increase remained low compared to the reference group CO, indicating the favourable sulphate resistance of CA addition up to 156 days.

For sample with WWB addition at 28 days, the mass increment was 1.023 % (17.9 % reduction), 0.989 % (20.93 % reduction), and 0.997 % (20.33 % reduction) for BC, CB, and CB2 respectively in comparison with the reference CO mix, being in good agreement with several studies [7,49]. Gupta et al. [7] reported that 2 wt% rice husk biochar led to 24 % reduction sulphate adsorption of biochar-cement mortar when compared to biochar-free samples at 28 days. However, samples with WWB addition only promoted a better reduction in water and sulphate adsorption than samples with CA addition only. As shown in Fig. 2, 80 % of WWB particle was smaller than 20 μm. The small size of pulverised

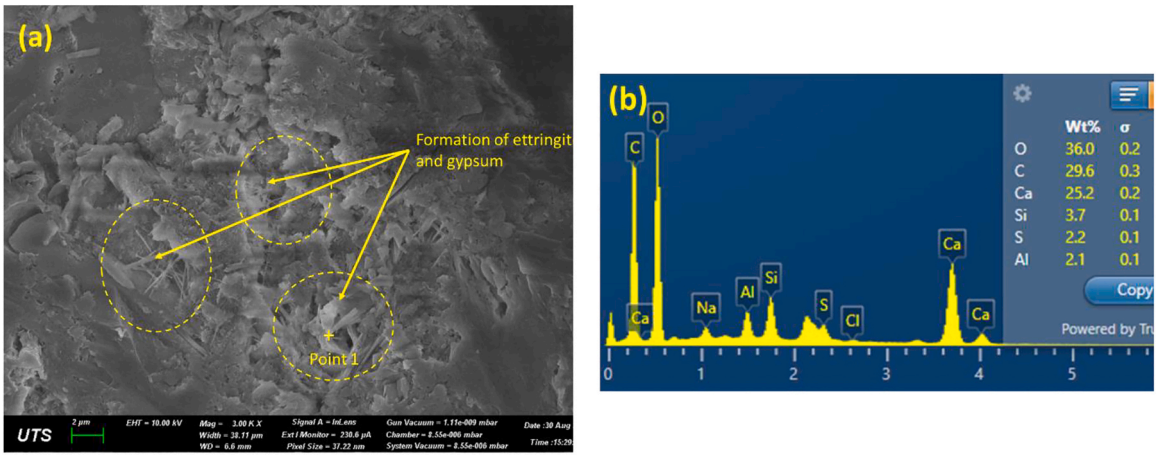

Fig. 7. (a) Formation of ettringite and gypsum in CO sample due to sulphate ingress at 28 days; (b) EDS result of ettringite formation at point 1.

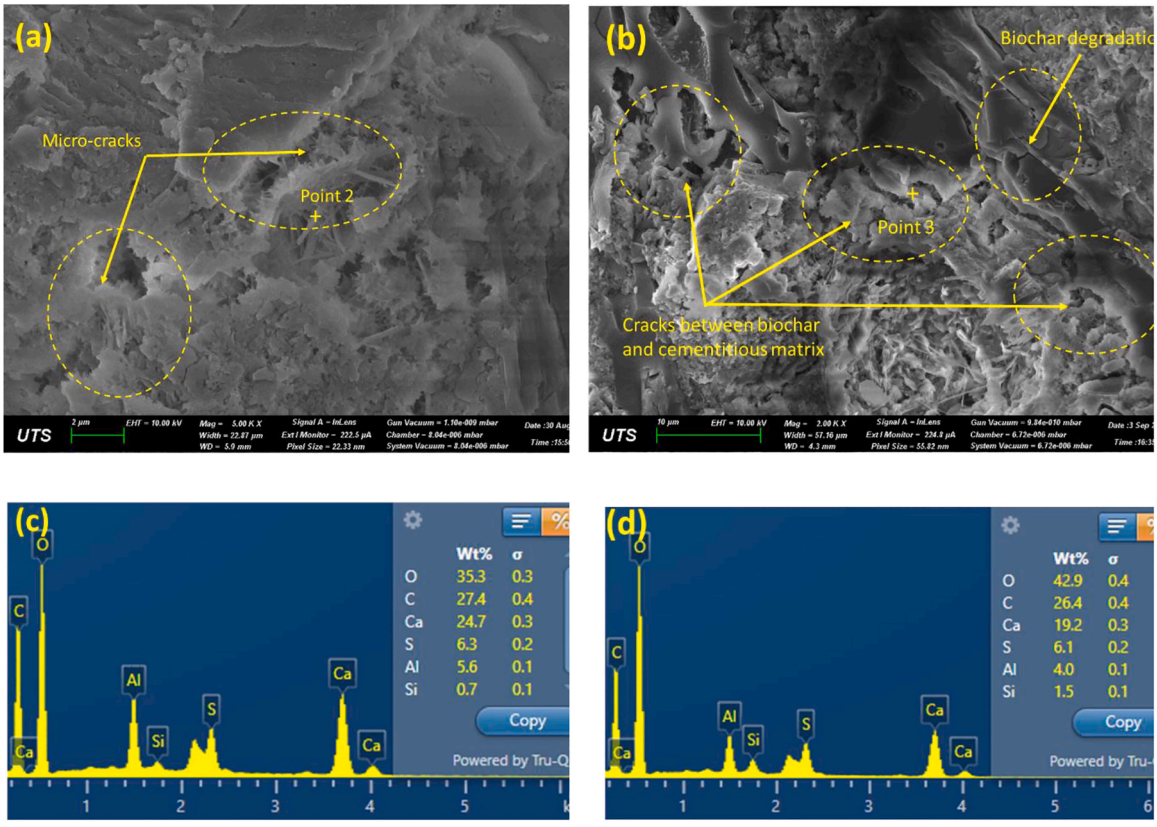

Fig. 8. (a) Micro-cracks in CA-cement matrix cured in Na_2SO_4 at 156 days; (b) Biochar degradation and cracks formed between biochar particle and the cementitious matrix in CB sample cured in Na_2SO_4 at 156 days; (c) EDS result of Point 2 in CA sample; (d) EDS result of Point 3 in CB sample.

WWB not only provided favourable filler effect improving the compactness of the biochar-cement matrix, but also improved local hydration by reducing the effective water-to-binder ratio before sulphate immersion. As a result, WWB addition promoted a slightly better sulphate resistance than CA addition at 28 days. However, it could be noted that the mass stabilised from 28 days to 96 days but increased from 96-day exposure to 156-day exposure for all samples. There was a significant increase of mass change rate for specimens with WWB after 120 days. Many studies [50,51] reported that, although pulverised biochar could improve sulphate resistance at early immersion age, long-term exposure inevitably induced micro-cracks in the cementitious matrix and the interfacial transition zone (ITZ) between biochar and the hydration product. The primary reaction products of sulphate attack are ettringite and gypsum based on the consumption of calcium hydroxide or calcium aluminate [7], causing porous microstructure. The evidence could be found in the SEM analysis of the CA samples (Fig. 8a) and CB samples (Fig. 8b) at 156-day exposure, where needle-shape ettringite induced significant cracks lowering the sulphate resistance. As depicted in Figs. 8c and 8d, the SEM-EDS results of point 2 in CA sample and point 3 in CB sample indicated the formation of ettringite in the cementitious matrix. Furthermore, due to the long-term sulphate immersion, biochar degradation and cracks in the ITZ of the biochar-cement matrix was also observed (Fig. 8b), creating additional channels for aggressive ions diffusion. As a result, WWB addition led to 16.14 %, 18.12 %, and

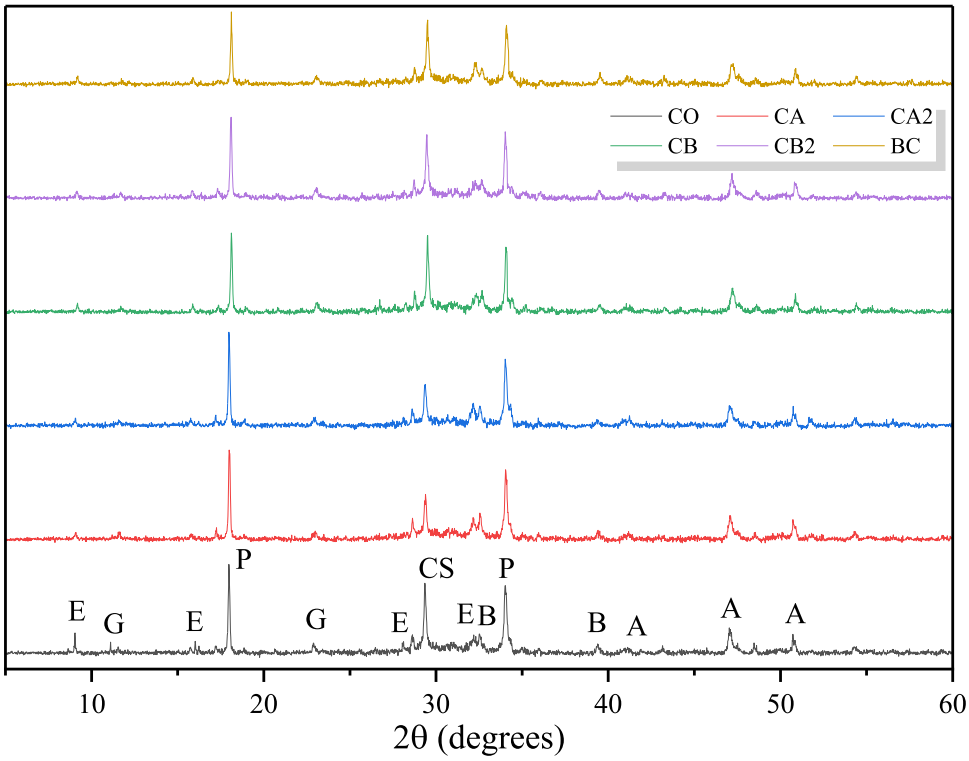

Fig. 9. XRD pattens of samples exposed to 156-day sulphate solution. (Note: A=alite; B=belite; CS= C-S-H; E = ettringite; G=gypsum; P = portlandite.

16.99 % reduction in 156-day sulphate solution adsorption when compared to the control group for BC, CB, and CB2 respectively.

Fig. 9 depicts the XRD pattens of crushed samples exposed to 5 % sodium sulphate in 156 days for all groups. According to Zhan et al. [52], diffraction peak at 2θ of 29.2° was identified as CS, and portlandite was found at 2θ of 18.1° and 34. 1°. Wang et al. [53] found gypsum at 2θ of 11.08° and 22.84° in the diffraction spectra. Ettringite was observed at 2θ of 9.1° and 16. 1° (Fig. 9). Boudache et al. [54] found additional ettringite peak at 2θ of 27.2°. Furthermore, unhydrated cement clinkers, such as alite and belite were observed in all groups.

However, it should be noted that XRD patten (black line) had higher diffraction peaks of ettringite and gypsum than other groups, being in a good agreement with mass change results (Fig. 6) The correlation is that due to the excessive formations of sulphate-attack products (ettringite and gypsum), more micro-cracks formed during the immersion period, creating more accessible channels for water and sulphate ions to penetrate into the cementitious matrix. As a result, higher formations of ettringite and gypsum led to higher sulphate solution absorption in the control group (Fig. 6). Regarding the presence of CA or WWB, although a denser microstructure was promoted at early age, sulphate ions inevitably penetrated into the cementitious matrix to form ettringite or gypsum for all groups at 156 days (Fig. 9).

Fig. 10 shows the mechanical strength degradations of all samples immersed in the 5 % sodium sulphate solution up to 156 days. 6.47 % increase in the flexural strength was observed for BC group when compared to CO group, which was higher than the 2 % strength increase observed on samples cured in water. This may be due to the formation of ettringite blocking the pores of WWB after 28-day of sulphate solution exposure, densifying the microstructures leading to an increase in flexural strength. It was evident from the precipitation of calcium hydroxide and ettringite in the pores of WWB (Fig. 11a), and the EDS results supported that there was formation of ettringite as the result of exposure to the Na_2SO_4 solution in Fig. 11(b). For samples with CA addition, the flexural strength increase was 8.44 %, 9.58 %, 7.81 %, and 8.79 % for CA group, CA2 group, CB group, and CB2 group respectively compared to CO mix at 28-day. Due to formations of ettringite and gypsum, at 28 days, samples cured in Na_2SO_4 solution had slightly higher mechanical strength than those of samples cured in water (Figs. 5a and 5b). Gupta et al. [7] explained that at early exposure age, ettringite and gypsum acted as pore filling products reducing the porosity of the cementitious microstructure, promoting the small increase in the mechanical strengths. For long-term sulphate exposure at 156 days, WWB addition only promoted 6.05 % increase in the flexural strength compared to CO group, and CA addition led to 14.7 %, 12.56 %, 10.13 % and 9.64 % flexural strength increase for CA, CA2, CB, and CB2 group respectively when compared to the reference group.

Regarding compressive strength, the addition of CA and WWB promoted better compressive strength than the reference group at all ages. At 28 days, CA addition led to 12.22 % and 10.53 % compressive strength increase, while 5 wt% WWB promoted 10.1 % increase in the compressive capacity when compared to CO group. Similar to the development of flexural strength, BC samples (10.1 % strength increase) cured in Na_2SO_4 solution had better strength increase than BC sample (6.5 % strength increase) cured in water at 28 days. The evidence could be observed in Fig. 11a, hydration products and formation of ettringite gradually filled the pores of WWB, leading to a denser biochar-cement matrix carrying more compressive loads. Hashem et al. [55] found that the strength increase in the first-month immersion was attributed to the formation of gypsum in the pores of the cementitious matrix. The combination of CA and WWB led to 11.47 % and 10.4 % compressive strength increase for CB and CB2 respectively. At 156-day of sulphate immersion, due to the continuous sulphate attack, unfavourable cracks and biochar degradation were observed (Figs. 8a and 8b), resulting in strength loss. When compared to compressive strength (76.14 MPa) of CO group at 156 days, there was 15.28 %, 12.62 %, 9.9 %, 10.03 %, and 12.53 % strength increase for CA, CA2, BC, CB, and CB2 respectively.

Although slight strength improvement was observed after 28-day of sulphate immersion, the long-term Na_2SO_4 solution immersion led to a strength degradation for all samples. However, at 156 days, 1 wt% CA could lead to 15.28 % compressive strength improvement compared to that of the control group, while using 5 wt% WWB replacing cement promoted 10.1 % compressive strength increase. Fig. 12 presents the

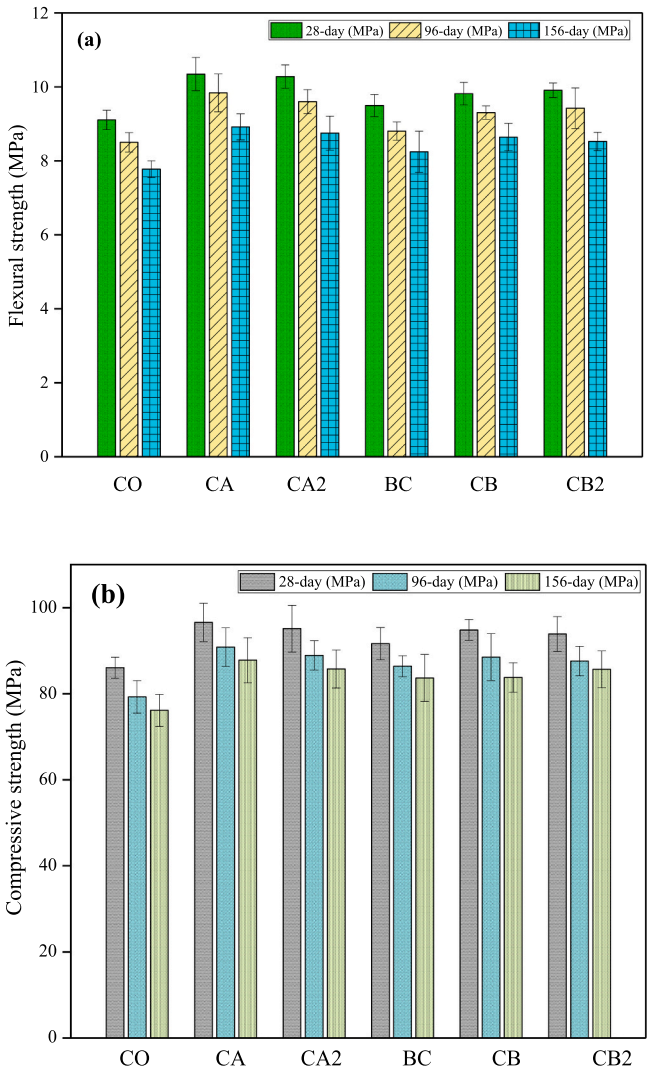

Fig. 10. Strength degradation of samples immersed inn 5 % Na_2SO_4 solution: (a) flexural strength, (b) compressive strength.

mechanical strength degradation rate of each group immersed in 5 % sodium sulphate solution from 28 days to 156 days. For flexural strength, 14.61 % strength degradation was found for CO group at 156 days, due to excessive cracks formation in the cementitious matrix. For CA addition only, 9.67 % and 12.29 % strength reduction were observed for CA and CA2 respectively. The denser CA-cement matrix led to lower strength reduction rate when compared to the control group. It should be noted that the presence of WWB seemed to lead to more strength degradation (11.98 – 14.95 %) than those of samples with CA addition only. As shown in Fig. 8b, cracks were observed in pulverised WWB including the ITZ, creating more accessible channels for aggressive ions (e.g. water and sulphates) to penetrate deeper into the cementitious matrix. As a result, higher strength reduction was found in samples with WWB. For compressive strength, it could be noted that a lower strength reduction rate was found for compressive strength degradation (Fig. 12). As mentioned in Section 3.1, compressive forces lead to voids and pores closure. Although excessive cracks were found in the cementitious matrix (Figs. 8a – 8b) at 156 days, the reduction rate was only 11.52 % for CO group. Similar to flexural strength degradation rate, the presence of WWB led to slightly higher compressive strength reduction rate (8.76 – 11.64 %) than those of samples with CA addition (9.1 – 9.85 %) (Fig. 12). Overall, samples with 1 wt% CA addition seemed to show the best resistance to mechanical strength degradation (Fig. 10a, Fig. 10b, and Fig. 12).

3.3. 5 % sodium chloride solution exposure

Fig. 13 shows the adsorption of NaCl solutions of all samples up to 156 days. The mass increase is generally greater than that of water adsorption (Fig. 4). While exposed to the NaCl solution, some chlorides were bound by hydration productions with aluminate phases to form Friedel's salt (FS), being $3CaO.Al_2O_3.CaCl_2{\cdot}10\ H_2O$. For WWB addition, BC, CB and CB2 showed 20.85 %, 23.23 %, and 22.1 % reduction on the mass increase respectively when compared to CO group. First of all, pulverised WWB could lead to a denser microstructure resisting chloride ingress into the cementitious matrix. Meanwhile, porous WWB provided additional zone for hydration products formed binding more chlorides, interfering their diffusion. It is evidenced by the formation of FS on the biochar pores (Figs. 14a – 14e). As shown in Fig. 14a at 10k magnification, WWB was bound with the cementitious matrix with hydration products binding FS filling in the pore after 28-day of NaCl immersion, confirmed by the EDS map scan in the BC sample (Figs. 14b – 14c). Fig. 13d depicts another evidence of WWB offering additional spaces for the formation of FS, confirmed by the EDS result in Fig. 14e. It should be noted that, although samples were immersed in 5 % NaCl solution after 28 days, denser hydration products could be observed (Fig. 14d), and this applied to other samples (SEM photos not shown). Similar observation was found by Qiao et al. [56], where FS formed at a slow speed,

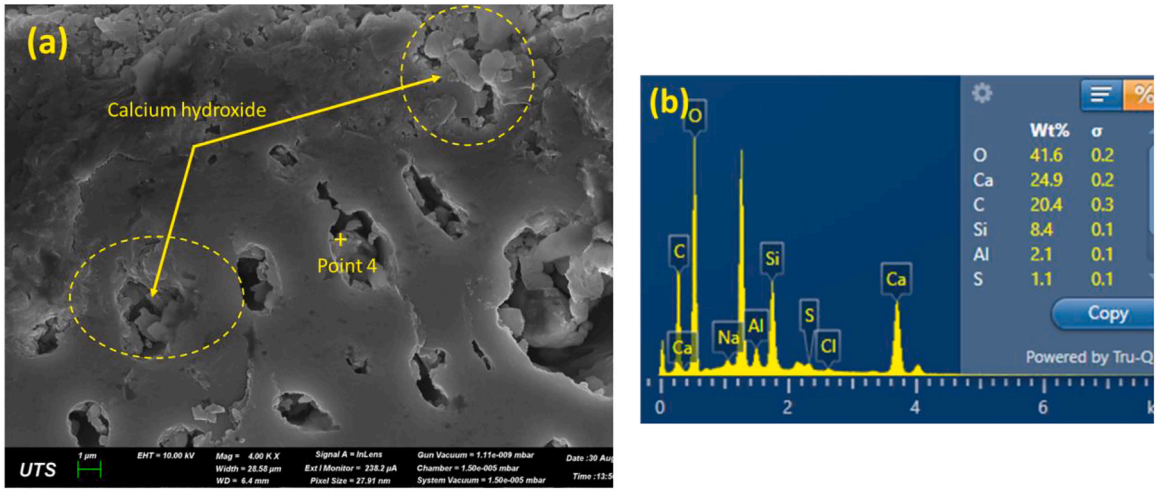

Fig. 11. (a) Hydration and sulphate attack products in biochar pore at 28 days; (b) EDS result of point 4 in CB samples cured in Na_2SO_4 at 28 days.

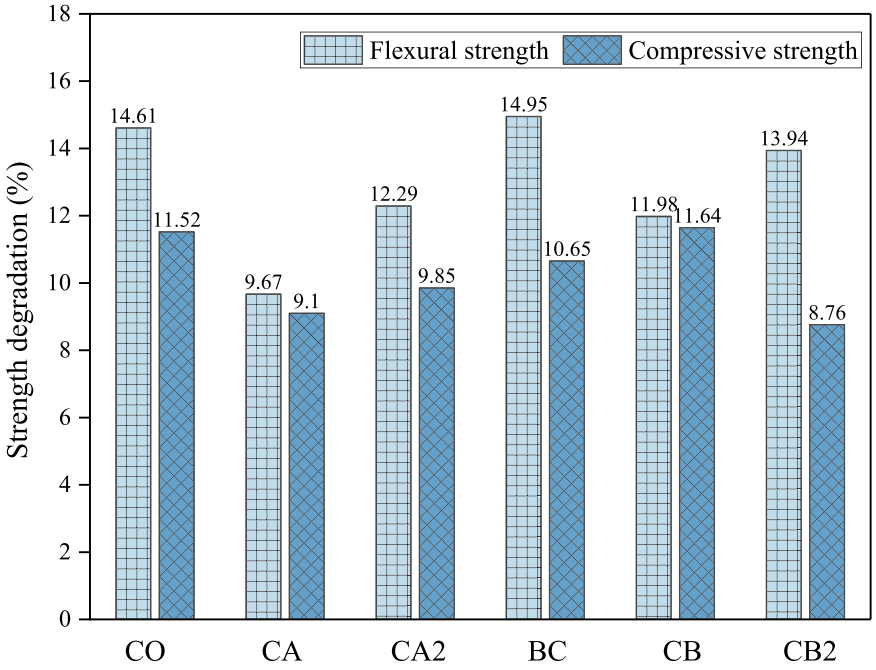

Fig. 12. Mechanical strength degradation rate of samples immersed in 5 % sodium sulphate solution at 156 days.

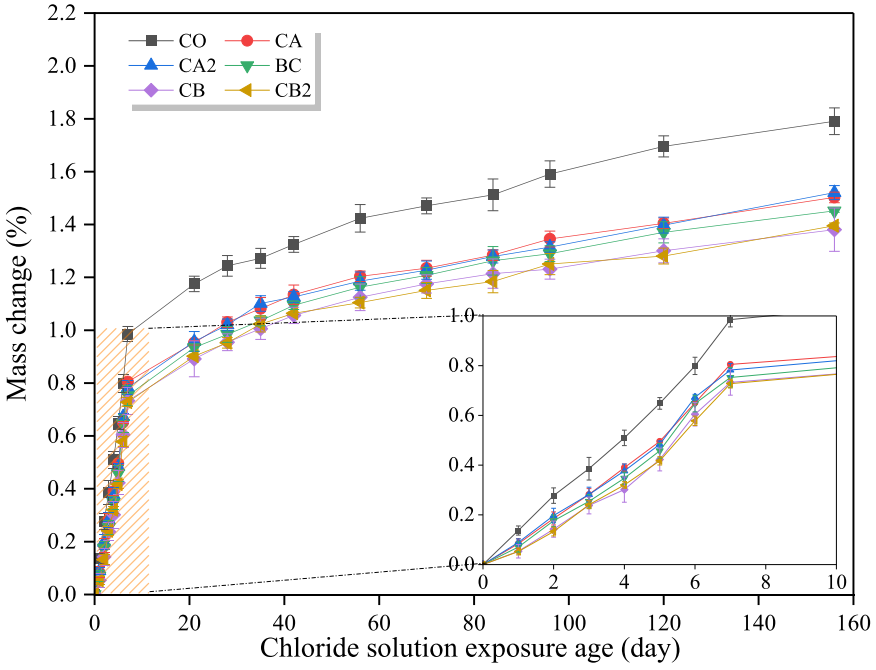

Fig. 13. Mass change of samples immersed in 5 % sodium chloride solution.

leading to less damage to the cementitious microstructure. In addition, CA addition promoted a reduction of 17.16 % and 18.1 % in mass increase for CA and CA2 group respectively when compared to the reference group. Overall, the combination of WWB and CA demonstrated the best chloride resistance after 28-day of immersion, due to a denser cementitious matrix (Figs. 14a and 14d).

However, after 60 days, Fig. 13 shows that the NaCl solution adsorption rate increased significantly. As shown in Fig. 14a, after 156-day of NaCl solution immersion, sodium ions replaced calcium ions leading to hydration product degradation and more porous microstructure (Figs. 15a and 15d), being consistent with the observation by Sugiyama [57]. Sugiyama [57] found that sodium ions replaced calcium ions in C-S-H gels, where exchange rated was enhanced for C-S-H with lower Ca/Si ratios. CA addition led to the adsorption rate reduction of 15.8 % and 15.2 % respectively for CA and CA2 samples when compared to CO group at 156 days. WWB addition led to a mass increase reduction of 17.8 %, 19.2 %, and 20.1 % for BC, CB, and CB2 group respectively at 156 days. It should be noted that, similar to WWB degradation at 156 days in the sodium sulphate immersion, WWB degradations were observed in CB samples at 156 days (Fig. 15d). According to the EDS spectrum in Fig. 15e, the high percentage of silica indicated that FS may be bound with C-S-H gel due to chloride-ion penetration, generating cracks in the ITZ of the biochar-cement matrix. Additionally, visible crack was found in the WWB particle, allowing more chlorides ions to

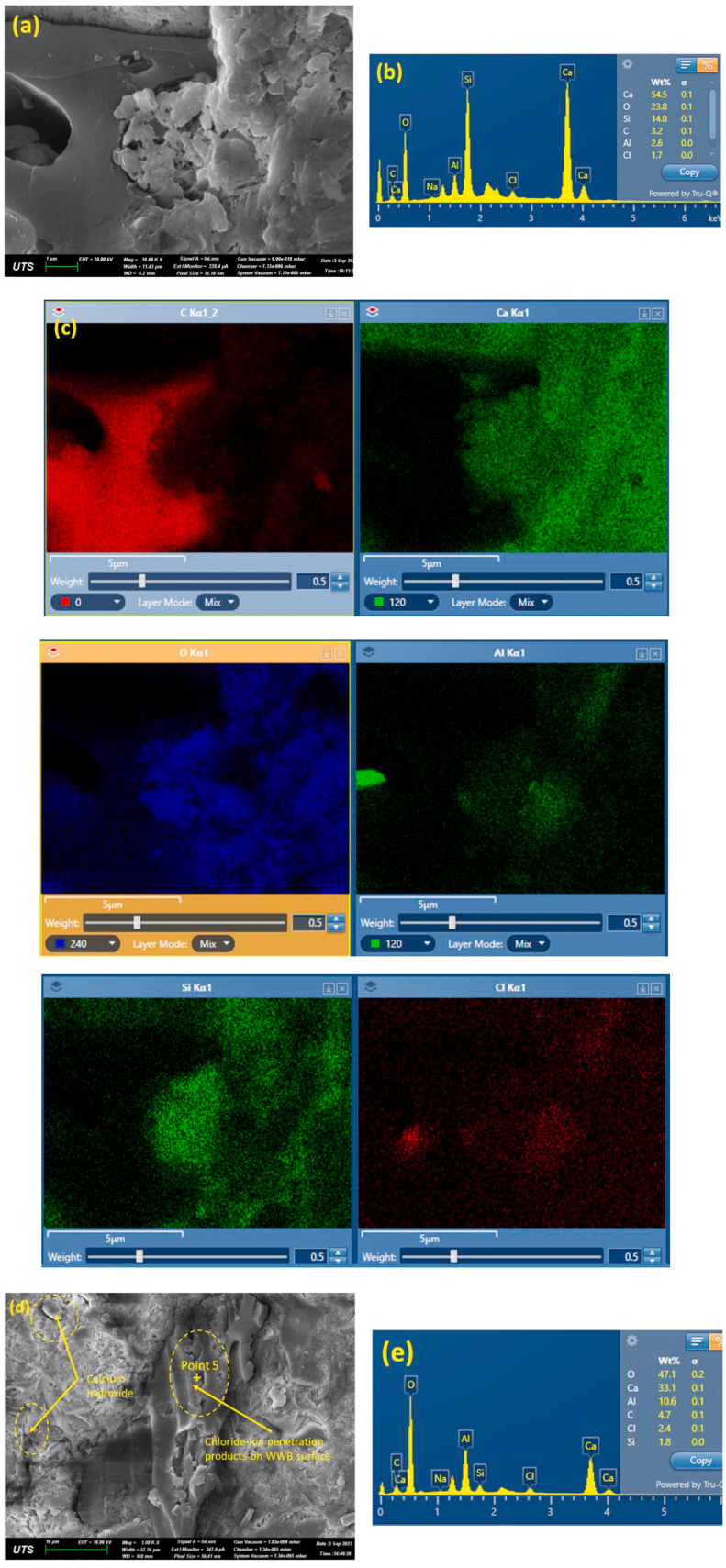

Fig. 14. (a) Chloride-ion penetration products in WWB pore of CB sample at 28 days; (b) EDS results of map scan; (c) Elemental distribution in map scan from (a); (d) Micro-cracks on the biochar-cement matrix and chloride-ion penetration products in WWB pore at 28 days; (e) EDS result of Point 5.

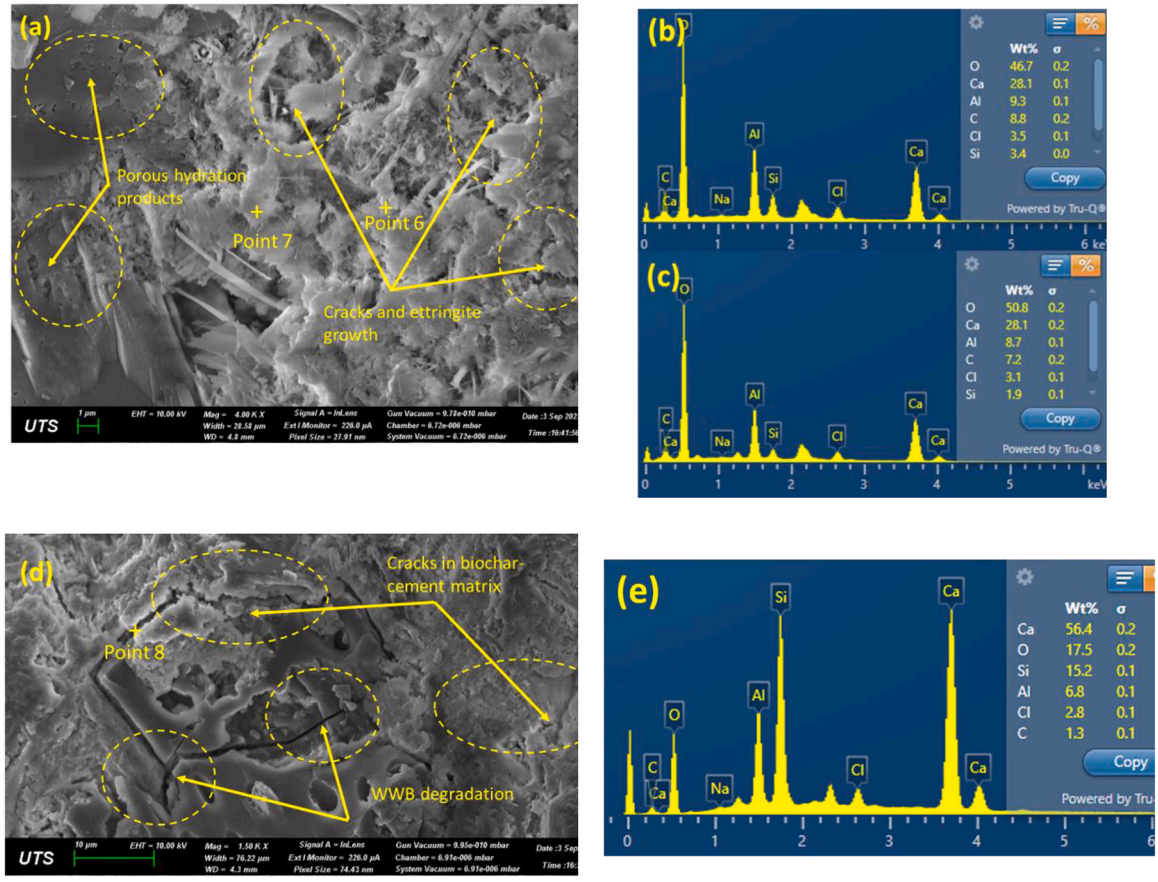

Fig. 15. (a) Excessive cracks on CO samples at 156 days; (b) EDS result of point 6; (c) EDS result of point 7; (d) WWB degradation on CB samples at 156 days; (e) EDS result of point 8.

penetrate into the cementitious matrix, being in good agreement with several other studies [7,58].

Fig. 16 presents the degradation of the mechanical strengths of the different groups immersed in 5 % NaCl solution up to 156 days. BC group showed a slight increase in the flexural strength (3.12 %) when compared to CO group, while CA addition led to 10.6 % and 8.8 % flexural strength increase for CA and CA2 respectively after 28-day of NaCl solution exposure. It should be noted that BC samples cured in Na_2SO_4 at 28 days showed 6.47 % flexural strength increase, being slightly higher than that of BC samples immersed in 5 % NaCl solution at 28 days. For CB and CB2 group, 4.86 % and 5.8 % flexural strength increase were observed at 28 days. At long-term immersion, the flexural strength of CO group achieved an average value of 7.04 MPa (156 days). When compared to the CO group, a strength increases of 18.5 % and 15.4 % was observed for CA (8.34 MPa) and CA2 group (8.13 MPa) respectively. In terms of WWB addition, when compared to the CO group, there was 10.12 % (7.75 MPa), 12.18 % (7.9 MPa), and 11.35 % (7.84 MPa) flexural strength increment was observed for BC, CB, and CB2 group respectively. As presented in Fig. 15d, excessive formations of FS and ettringite led to cracks in the ITZ of the biochar-cement matrix, allowing more chlorides to penetrate into the cementitious microstructure, lowering the flexural strength.

When compared to CO group, CA promoted 12.36 % and 9.5 % compressive strength increase, and WWB led to 5.4 %, 9.11 %, and 8.1 % compressive strength increase for BC, CB, and CB2 respectively at 28-day NaCl solution immersion. A slightly higher increase in compressive strength was observed when compared to flexural strength for BC group, as already discussed in Section 3.1. Fig. 14a shows the degradation of hydration products and excessive formation of ettringite and FS in CO specimens, leading to micro-cracking. As a result, there were significant strength loss for all samples after 156-day of NaCl solution exposure. The compressive strength of CA groups was 17.6 % and 16.2 % strength higher than that of CO group at 156 days, while WWB addition led to 7.65 %, 12.01 %, and 10.46 % compressive strength increase for BC, CB, and CB2 respectively. Considering the slight increase in the 156-day compressive strength, the combination of CA and WWB had favourable long-term effect on the resistance against chloride-ion exposure.

Fig. 17 presents the mechanical strength degradation rate of each group immersed in 5 % sodium chloride solution from 28 days to 156 days. For flexural strength degradation, the highest degradation rate was found for CO group (22.39 %), significantly higher than that of the other samples. As depicted in Fig. 15a, numerous cracks allowed more chloride ions and water to penetrate into the cementitious matrix, lowering the flexural strength. Only 16.92 – 17.75 % strength reduction was observed for CA specimens, indicating lower the strength reduction rate of the CA-cement composites due to the denser microstructure. The presence of WWB led to a similar flexural strength reduction rate (16.99 – 18.36 %) when compared to CA samples. In terms of compressive strength reduction, a lower reduction rate was observed for all groups when compared to flexural strength. Amin et al. [59] reported that 13.96 % compressive strength reduction after 4 months of chloride immersion. They found that chloride ingress led to micro-crack formations reducing compressive strength, including the formation of Friedel's salt. The addition of CA led to the lowest compressive strength reduction rate of 11.13 – 12.34 %, while 5 wt% WWB slightly increased the strength degradation rate, being 14.47 %, 14.04 %, and 14.39 % for BC, CB, and CB2 group respectively. It should be noted that the degradation of WWB in long-term chloride immersion was the primary reason for the negative impact on the strength development.

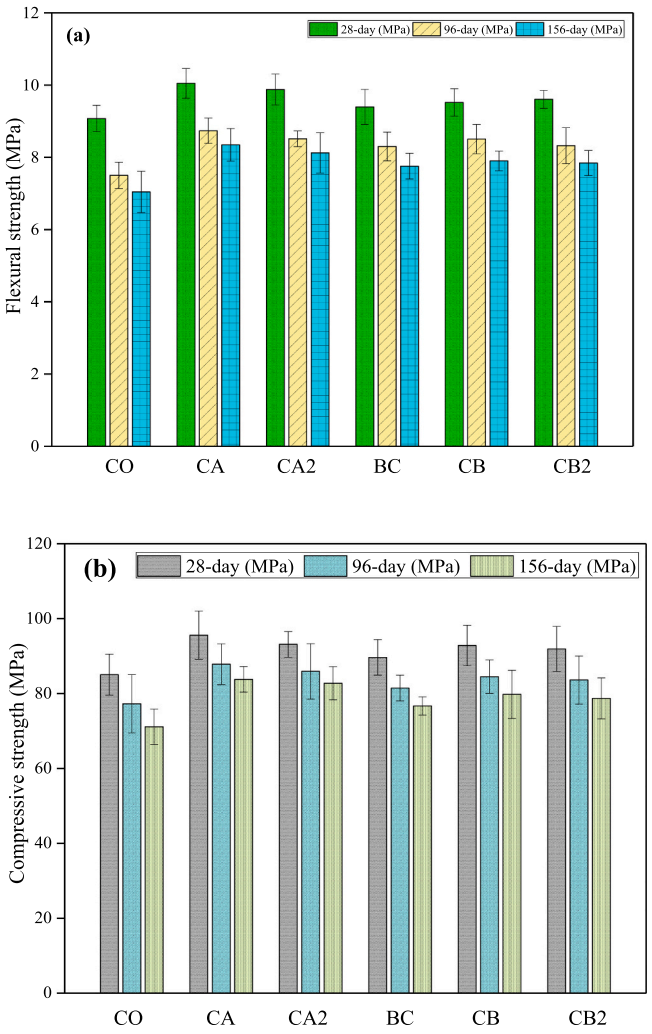

Fig. 16. Strength degradations in 5 % NaCl solution: (a) flexural strength, (b) compressive strength.

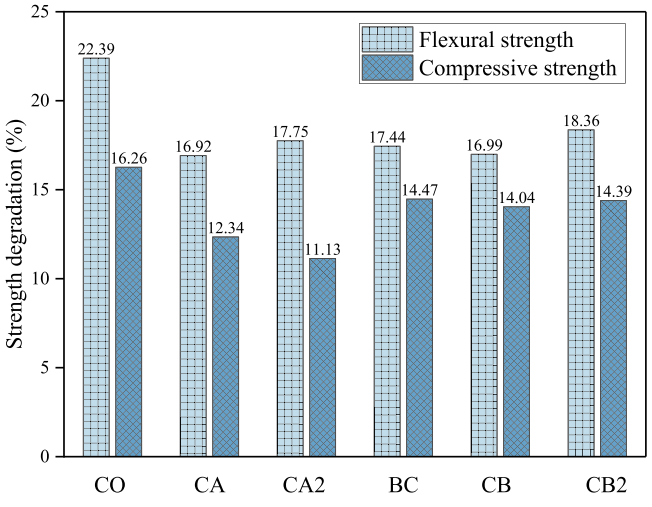

Fig. 17. Strength degradation rate immersed in 5 % sodium chloride solution at 156 days.

4. Discussion

Before the immersion of the specimens in the solutions, e.g. water, Na_2SO_4, or NaCl, all samples were cured in a conditioned chamber with 95 ± 5 % relative humidity and 23 ± 2 °C for 3 days. As a result, all samples achieved a sufficient compressive strength higher 20 MPa following the curing protocol. As presented in Fig. 18 and Fig. 19, at 0-day immersion, CA induced formation of crystalline deposit to block small pores and partially fill in relatively large pores. Similarly, small pulverised WWB completely filled the small pore, and large WWB bound with the cementitious matrix (Fig. 11a, Fig. 13a, and Fig. 13d). In this case, both CA and WWB formed a primary barrier in major pores limiting the access of water and aggressive ions to penetrate.

4.1. Sulphate ingress

In terms of time-dependent sulphate ingress, cracks were formed due to formation of ettringite after 28-day sulphate immersion (Fig. 7a), allowing sulphate solution to penetrate into the cementitious matrix to generate more cracks. However, CA induced crystalline deposits in the large capillary pore to form a denser CA-cement matrix (Fig. 18b2), limiting the access of sulphates. Thus, samples with CA performed better than CO group after 28-day of Na_2SO_4 immersion. WWB addition had a slightly different way in limiting the sulphate ingress. As show in Fig. 18b2, small pulverised WWB particle filled the pores while large WWB offered additional sites for the formation of ettringite (Fig. 11a), reducing the internal stress in the cementitious matrix. Similar finding was reported by Gupta et al. [7]. They observed that biochar offered more internal pores for the formation of sulphate attack reaction products, mitigating the potential threat of microstructural cracks in the biochar-cement composite. After 156-day Na_2SO_4 immersion, Fig. 18a3 depicts excessive cracks and formation of ettringite in the cementitious matrix. Without the presence of CA and WWB, sulphate ions could directly penetrate into the matrix via the existing cracks to form new cracks. In particular, cracks connected the pores in the cementitious matrix, significantly increasing the sulphate adsorption at 156 days (Fig. 6). As shown in Fig. 18b3, due to continuous sulphate ingress, cracked formed in the protective barrier of crystalline deposit. As a result, sulphate solution could penetrate into the cementitious matrix behind the pores with crystalline deposits to form more ettringites and cracks. However, the difference in crack depth observed in Fig. 18a3 and Fig. 18b3 provided evidence for the reduction of sulphate solution adsorption by CA addition. Similarly, as shown in Fig. 18c3, sulphate ingress led to the degradation of WWB and the formation of cracks in the ITZ (Fig. 8b). Hence, sulphates could penetrate into the cementitious matrix through pores initially blocked by WWB, leading to additional cracks further lowering the strength and increasing the sulphate solution adsorption.

4.2. Chloride-ion penetration

After 28-day of NaCl solution immersion, the formation of FS and ettringite could be observed in Fig. 19a2. Since CA promoted additional crystalline deposits blocking the pores, the formation of FS did not damage the protective crystalline layer, and cracks only formed in front of the pores with crystalline deposit. As discussed in Section 3.3, due to the relatively large size of FS (up to 28 μm), FS formed on the surface of the WWB, confirmed by map scan (Fig. 14b) and point scan (Fig. 14e). Thus, chloride solution did not pass through WWB particle after 28-day of NaCl solution immersion, limiting the continuous growth of FS and ettringite stimulating the crack formation. The major difference with in Na_2SO_4 solution at 28 days was that there was ettringite formation growth in WWB's pore, and FS formed on the surface of WWB particle. However, both CA and WWB created effective barriers to mitigate aggressive-ion ingress.

After 156-day NaCl solution immersion, excessive cracks were

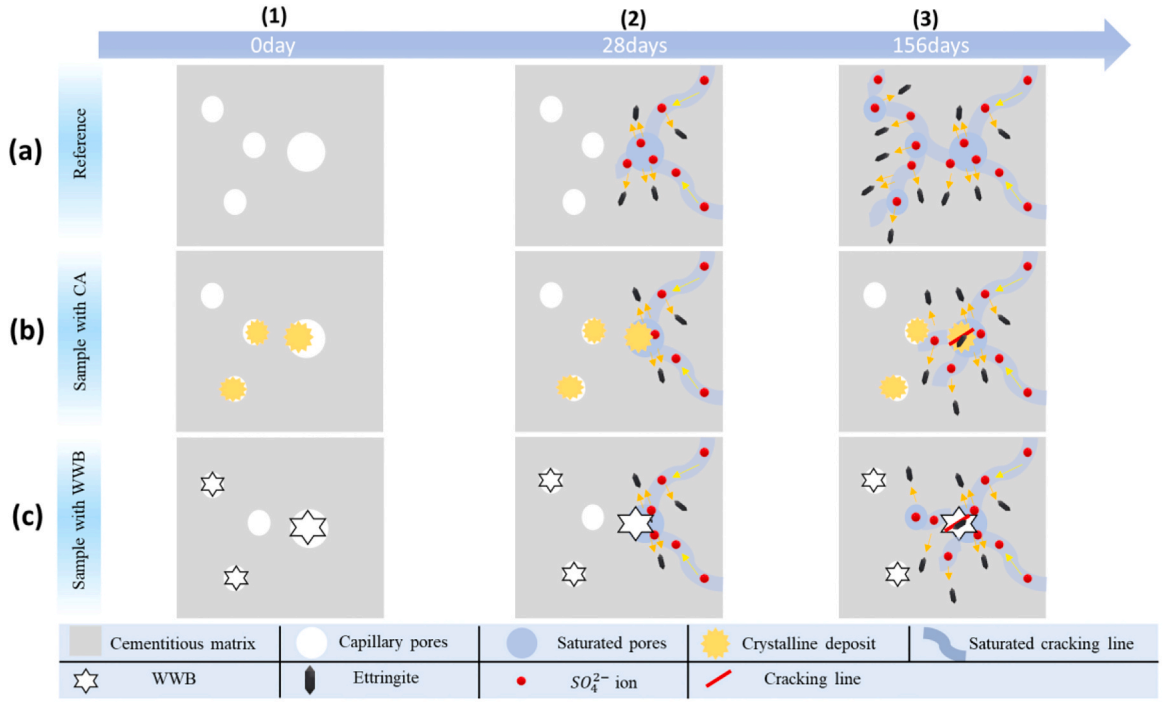

Fig. 18. Schematic showing time-dependent sulphate ingress up to 156 days: (a) Reference group; (b) Samples with CA addition; (c) Samples with WWB addition.

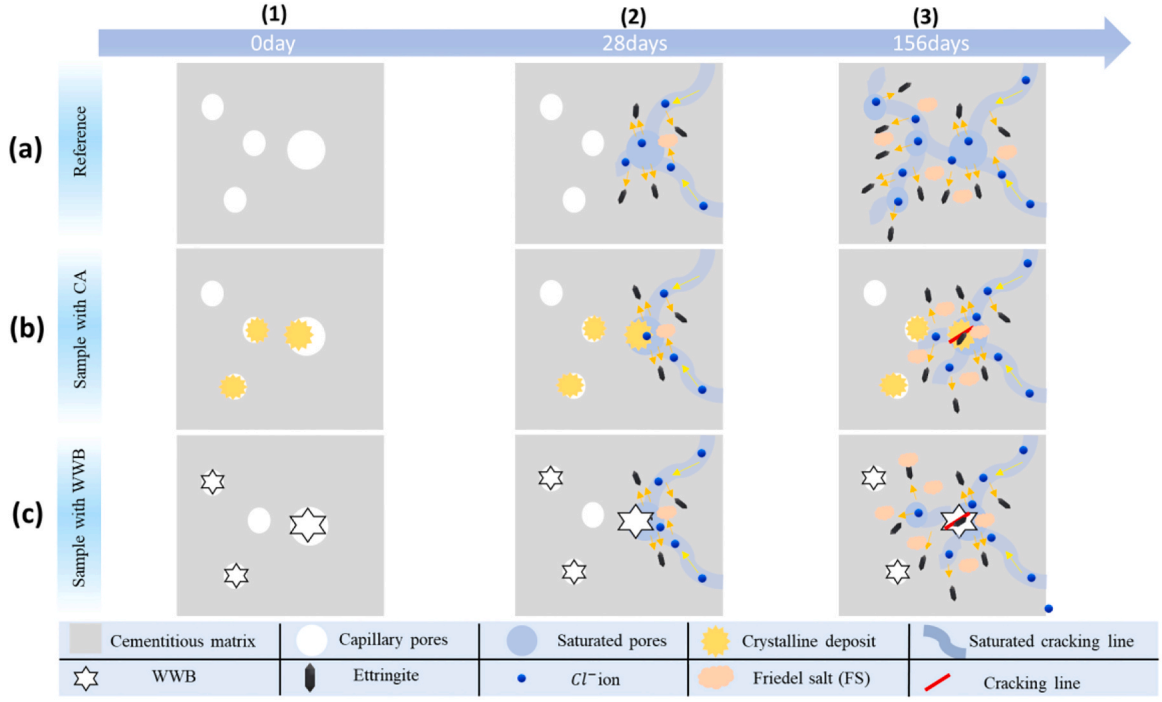

Fig. 19. Schematic showing time-dependent chloride-ion penetration up to 156 days: (a) Reference group; (b) Samples with CA addition; (c) Samples with WWB addition.

observed in CO group (Fig. 15a). FS and ettringite formed in large pore creating high tensile stress to the cementitious matrix, leading to crack growth around the large pore leading to more channels for chloride ingress (Fig. 19a3). It should be noted that although CA addition induced crystalline deposit partially filling the large pores (Fig. 19b3), continuous chloride ingress led to cracks in the protective layer of crystalline deposit. Thus, chloride ions penetrated deeper into the cementitious matrix, resulting in additional formations of FS and ettringite in capillary pores. At 156 days, WWB degradation was also observed due to the excessive formation of FS and ettringite (Fig. 15d). As a result, aggressive ions and water could penetrate via the cracks through the ITZ and WWB, causing new cracks behind the pore with WWB (Fig. 19c3). However, although chlorides broke the protective barrier by CA and WWB, effective chloride resistance could be still achieved, evidenced by the strength increase when compared to the reference group (Figs. 10a - 10b and Figs. 16a – 16b).

Overall, the presence of CA and WWB improves both sulphate and chloride resistance as well as the mechanical strength and reducing solutions adsorption. The primary benefit of CA addition in improving durability properties lied on the crystalline deposit densifying the cementitious matrix, particularly in large pores (Fig. 18b1 and Fig. 19b1). In the early immersion age up to 28-day, crystalline deposit acted as protective layer limiting the access of sulphate and chloride ions. Furthermore, there were two advantages of WWB addition in improving the durability properties of the biochar-cement composites. Firstly, small pulverised WWB filled the small pores densifying the microstructure. Secondly, large WWB offered additional space for ettringite (Fig. 11a) and FS formation (Fig. 14a), reducing the tensile stress in the matrix and delaying crack development. However, both protective layers seemed to be broken due to excessive formations of sulphate and chloride ingress products at 156 days (Fig. 8b and Fig. 15d), leading to cracks in the deeper cementitious matrix. However, the compressive strength and flexural strength of composites containing WWB were still higher than reference mix CO at 156 days, being in good agreement with Lin et al. [17].

5. Conclusions

This study conducted long-term immersion test investigating the effects of CA and WWB addition on the long-term resistance performance in Na_2SO_4 and NaCl solutions up to 156 days. The finding of this study conservatively concluded that the addition of CA and WWB could improve the durability properties of coastal structures immersed in sea water. The main findings are as the follows:

(1) CA and WWB addition reduced the water adsorption due to a denser microstructure while curing in water up to 156 days. CA addition promoted 6.8–7.3 % and 10.5 – 12.2 % increase in flexural strength and compressive strength respectively for the cementitious composites after 28-day of water exposure. For WWB addition only, similar flexural strength and slight increase in compressive strength (6.5 %) was observed for BC samples at 28 days. The combination of CA and WWB addition led to 6.3 – 6.9 % and 9.22 – 10.4 % strength increase in flexural strength and compressive strength respectively at 28 days.
(2) Compared to the control group, CA addition led to 15.1–16.2 % and 14.06 – 14.7 % reduction in 28-day and 156-day Na_2SO_4 solution adsorption respectively. Similar findings were observed for samples with WWB. 5 wt% WWB led to 17.9 – 20.93 % and 16.14 – 18.12 % reduction in sulphate solution adsorption at 28 days and 156 days respectively.
(3) XRD results suggested that higher amount of ettringite and gypsum formed in CO groups when compared to other groups after 156 days.
(4) Regarding strength degradation in the 5 % Na_2SO_4 solution after immersion for up to 156 days, both CA and WWB promoted a slight increase in mechanical strength when compared to CO group. Although CA and WWB led to a denser microstructure as protective layer against sulphate ingress at 28 days, cracks were still observed after 156 days of immersion the Na_2SO_4 solution, increasing solution adsorption and lowering mechanical properties.
(5) CA addition led to 17.16 – 18.1 % and 15.2–15.8 % reduction in NaCl solution adsorption at 28 days and 156 days respectively when compared to control group. Furthermore, WWB addition promoted 20.85 – 23.23 % and 17.8 – 20.1 % chloride solution adsorption reduction at 28 days and 156 days respectively.
(6) CA and WWB addition led to less compressive strength degradation in NaCl solution up to 156 days. CA promoted 8.8 – 10.6 % and 15.4 – 18.5 % flexural strength increase when compared to control group at 28 days and 156 days respectively and led to 9.5–12.36 % and 16.2 – 17.6 % compressive strength increase after 28-day and 156-day of NaCl solution immersion respectively.
(7) Overall, CA and WWB led to a significant improvement against chloride-ion ingress maintaining higher mechanical properties than the reference group. Based on the discussions in Sections 3.2 – 3.3, 1 wt% CA addition promoted the best resistance against sulphate and chloride ingress, considering both strength comparison at both 28 days and 156 days and strength degradation rate at 156 days.
(8) Due to of the push worldwide for developing sustainable concrete and the increased manufacture of biochar, more studies are highly required to explore the performance of bio-char cementitious composites including shrinkage and durability properties such as carbonation or alkali-silica reaction.

CRediT authorship contribution statement

Arnaud Castel: Writing – review & editing, Project administration, Investigation, Funding acquisition. **Yu Pang:** Writing – review & editing, Investigation. **Zhizhong Deng:** Writing – review & editing, Investigation. **Tianxing Shi:** Writing – review & editing, Investigation. **Wengui Li:** Writing – review & editing, Investigation. **Vivian W.Y. Tam:** Writing – review & editing, Investigation. **Xuqun Lin:** Writing – original draft, Visualization, Validation, Software, Methodology, Investigation, Formal analysis, Data curation, Conceptualization. **Quang Dieu Nguyen:** Writing – review & editing, Supervision, Resources, Methodology, Investigation.

Declaration of Competing Interest

The authors declare that they have no known competing financial interests or personal relationships that could have appeared to influence the work reported in this paper.

Acknowledgements

The authors would like to appreciate Australian Research Council (DP220101051), Australia and the supports from University of Technology Sydney Research Academic Program at Tech Lab (UTS RAPT).

Data availability

Data will be made available on request.

References

[1] S. Lu, P. Zhao, C. Liang, L. Liu, Z. Qin, S. Wang, P. Hou, L. Lu, Utilization of Polydimethylsiloxane (PDMS) in polymer cement-based coating to improve marine environment service performance, Constr. Build. Mater. 367 (2023) 130359.
[2] A.M. Rashad, A.S. Ouda, Effect of tidal zone and seawater attack on high-volume fly ash pastes enhanced with metakaolin and quartz powder in the marine environment, Microporous Mesoporous Mater. 324 (2021) 111261.
[3] P. Li, W. Li, K. Wang, J.L. Zhou, A. Castel, S. Zhang, S.P. Shah, Hydration of Portland cement with seawater toward concrete sustainability: phase evolution and thermodynamic modelling, Cem. Concr. Compos. 138 (2023) 105007.
[4] P. Li, W. Li, K. Wang, H. Zhao, S.P. Shah, Hydration and microstructure of cement paste mixed with seawater – an advanced investigation by SEM-EDS method, Constr. Build. Mater. 392 (2023) 131925.
[5] M.Fathima Suma, M. Santhanam, A.V. Rahul, The effect of specimen size on deterioration due to external sodium sulphate attack in full immersion studies, Cem. Concr. Compos. 114 (2020) 103806.
[6] S. Ghorbani, I. Taji, M. Tavakkolizadeh, A. Davodi, J. de Brito, Improving corrosion resistance of steel rebars in concrete with marble and granite waste dust as partial cement replacement, Constr. Build. Mater. 185 (2018) 110–119.
[7] S. Gupta, S. Muthukrishnan, H.W. Kua, Comparing influence of inert biochar and silica rich biochar on cement mortar – hydration kinetics and durability under chloride and sulfate environment, Constr. Build. Mater. 268 (2021) 121142.
[8] L.G. Li, J.Y. Zheng, P.L. Ng, J. Zhu, A.K.H. Kwan, Cementing efficiencies and synergistic roles of silica fume and nano-silica in sulphate and chloride resistance of concrete, Constr. Build. Mater. 223 (2019) 965–975.

[9] J. Wen, B. Wang, Z. Dai, X. Shi, Z. Jin, H. Wang, X. Jiang, New insights into the green cement composites with low carbon footprint: the role of biochar as cement additive/alternative, Resour., Conserv. Recycl. 197 (2023) 107081.
[10] X. Li, F. Xu, B. Chen, B. Li, Z. Chen, J. Zhu, C. Peng, J. Lin, Investigation on the chloride ion erosion mechanism of cement mortar in coastal areas: from experiments to molecular dynamics simulation, Constr. Build. Mater. 350 (2022) 128810.
[11] Y. Jianming, W. Luming, J. Cheng, S. Dong, Effect of fly ash on the corrosion resistance of magnesium potassium phosphate cement paste in sulfate solution, Constr. Build. Mater. 237 (2020) 117639.
[12] X. Hu, C. Shi, J. Li, Z. Wu, Chloride migration in cement mortars with ultra-low water to binder ratio, Cem. Concr. Compos. 118 (2021) 103974.
[13] P. Chen, B. Ma, H. Tan, X. Liu, T. Zhang, C. Li, Q. Yang, Z. Luo, Utilization of barium slag to improve chloride-binding ability of cement-based material, J. Clean. Prod. 283 (2021) 124612.
[14] J.O. Ukpata, P.A.M. Basheer, L. Black, Slag hydration and chloride binding in slag cements exposed to a combined chloride-sulphate solution, Constr. Build. Mater. 195 (2019) 238–248.
[15] S. Song, Z. Liu, G. Liu, X. Cui, J. Sun, Application of biochar cement-based materials for carbon sequestration, Constr. Build. Mater. 405 (2023) 133373.
[16] X. Zhu, Y. Zhang, L. Chen, L. Wang, B. Ma, J. Li, C.S. Poon, D.C.W. Tsang, Bonding mechanisms and micro-mechanical properties of the interfacial transition zone (ITZ) between biochar and paste in carbon-sink cement-based composites, Cem. Concr. Compos. 139 (2023) 105004.
[17] X. Lin, W. Li, Y. Guo, W. Dong, A. Castel, K. Wang, Biochar-cement concrete toward decarbonisation and sustainability for construction: characteristic, performance and perspective, J. Clean. Prod. 419 (2023) 138219.
[18] M.Haris Javed, M. Ali Sikandar, W. Ahmad, M. Tariq Bashir, R. Alrowais, M. Bilal Wadud, Effect of various biochars on physical, mechanical, and microstructural characteristics of cement pastes and mortars, J. Build. Eng. 57 (2022) 104850.
[19] A. Sirico, P. Bernardi, B. Belletti, A. Malcevschi, E. Dalcanale, I. Domenichelli, P. Fornoni, E. Moretti, Mechanical characterization of cement-based materials containing biochar from gasification, Constr. Build. Mater. 246 (2020) 118490.
[20] G. Mishra, P. Danoglidis, S.P. Shah, M. Konsta-Gdoutos, Optimization of biochar and fly ash to improve mechanical properties and CO2 sequestration in cement mortar, Constr. Build. Mater. 392 (2023) 132021.
[21] F. Qu, Y. Zhang, X. Zhu, W. Xu, C.S. Poon, W. Li, D.C.W. Tsang, Roles of wood waste biochar for chloride immobilization in GGBS-blended cement composites, Constr. Build. Mater. 411 (2024) 134389.
[22] Y. Xie, H. Wang, Y. Guo, C. Wang, H. Cui, J. Xue, Mechanical performance and water resistance of biochar admixture lightweight magnesium oxychloride cement, Sci. Total Environ. 912 (2024) 168773.
[23] H. Maljaee, H. Paiva, R. Madadi, L.A.C. Tarelho, M. Morais, V.M. Ferreira, Effect of cement partial substitution by waste-based biochar in mortars properties, Constr. Build. Mater. 301 (2021) 124074.
[24] K.K. Weththasinghe, A. Akash, T. Harding, M. Subhani, M. Wijayasundara, Carbon footprint of wood and plastic as packaging materials – an Australian case of pallets, J. Clean. Prod. 363 (2022) 132446.
[25] Q. Al-Kaseasbeh, M. Al-Qaralleh, Valorization of hydrophobic wood waste in concrete mixtures: Investigating the micro and macro relations, Results Eng. 17 (2023) 100877.
[26] E. Tsampali, M. Stefanidou, The role of crystalline admixtures in the long-term healing process of fiber-reinforced cementitious composites (FRCC), J. Build. Eng. 60 (2022) 105164.
[27] H.-F. Li, Q.-Q. Yu, K. Zhang, X.-Y. Wang, Y. Liu, G.-Z. Zhang, Effect of types of curing environments on the self-healing capacity of mortars incorporating crystalline admixture, Case Stud. Constr. Mater. 18 (2023) e01713.
[28] C. Xue, W. Li, F. Qu, Z. Sun, S.P. Shah, Self-healing efficiency and crack closure of smart cementitious composite with crystalline admixture and structural polyurethane, Constr. Build. Mater. 260 (2020) 119955.
[29] P. Azarsa, R. Gupta, A. Biparva, Assessment of self-healing and durability parameters of concretes incorporating crystalline admixtures and Portland limestone cement, Cem. Concr. Compos. 99 (2019) 17–31.
[30] L. Wang, G. Zhang, P. Wang, S. Yu, Effects of fly ash and crystalline additive on mechanical properties of two-graded roller compacted concrete in a high RCC arch dam, Constr. Build. Mater. 182 (2018) 682–690.
[31] X. Hu, J. Xiao, Z. Zhang, C. Wang, C. Long, L. Dai, Effects of CCCW on properties of cement-based materials: A review, J. Build. Eng. 50 (2022) 104184.
[32] K. Zheng, X. Yang, R. Chen, L. Xu, Application of a capillary crystalline material to enhance cement grout for sealing tunnel leakage, Constr. Build. Mater. 214 (2019) 497–505.
[33] Y. Ding, Z. Wu, Q. Huang, Q. Wang, Q. Ren, Z. Zhang, J. Zhang, K. Huang, Research on crystalline admixtures for low carbon buildings based on the self-healing properties of concrete, Constr. Build. Mater. 409 (2023) 133932.
[34] X. Wang, Z. Yang, C. Fang, N. Han, G. Zhu, J. Tang, F. Xing, Evaluation of the mechanical performance recovery of self-healing cementitious materials–its methods and future development: a review, Constr. Build. Mater. 212 (2019) 400–421.
[35] J. Michael, S.H. Smith, S.A. Durham, M.G. Chorzepa, Crack control in concrete walls through novel mixture design, full-scale testing, and finite element analysis, Constr. Build. Mater. 166 (2018) 301–314.
[36] K. Aspiotis, K. Sotiriadis, A. Ntaska, P. Mácová, E. Badogiannis, S. Tsivilis, Durability assessment of self-healing in ordinary Portland cement concrete containing chemical additives, Constr. Build. Mater. 305 (2021) 124754.
[37] X. Lin, W. Li, A. Castel, T. Kim, Y. Huang, K. Wang, A comprehensive review on self-healing cementitious composites with crystalline admixtures: design, performance and application, Constr. Build. Mater. 409 (2023) 134108.
[38] C. Xue, Performance and mechanisms of stimulated self-healing in cement-based composites exposed to saline environments, Cem. Concr. Compos. 129 (2022) 104470.
[39] C. Xue, W. Li, Z. Luo, K. Wang, A. Castel, Effect of chloride ingress on self-healing recovery of smart cementitious composite incorporating crystalline admixture and MgO expansive agent, Cem. Concr. Res. 139 (2021) 106252.
[40] A. Pawar, N.L. Panwar, A comparative study on morphology, composition, kinetics, thermal behaviour and thermodynamic parameters of Prosopis juliflora and its biochar derived from vacuum pyrolysis, Bioresour. Technol. Rep. 18 (2022) 101053.
[41] A.Sf Testing, M.C.C.-o Cement, ASTM C348-21: standard Test Method for Flexural Strength of Hydraulic-Cement Mortars, ASTM International, 2013.
[42] A. Standard, ASTM C349-18: standard test method for compressive strength of hydraulic-cement mortars (using portions of prisms broken in flexure), Annu. Book ASTM Stand. (2018) 1–4.
[43] C. Qiao, W. Ni, Q. Wang, J. Weiss, Chloride diffusion and wicking in concrete exposed to NaCl and MgCl2 solutions, J. Mater. Civ. Eng. 30 (3) (2018) 04018015.
[44] G. Li, S. Liu, M. Niu, Q. Liu, X. Yang, M. Deng, Effect of granulated blast furnace slag on the self-healing capability of mortar incorporating crystalline admixture, Constr. Build. Mater. 239 (2020) 117818.
[45] S. Gupta, H.W. Kua, S.D. Pang, Biochar-mortar composite: manufacturing, evaluation of physical properties and economic viability, Constr. Build. Mater. 167 (2018) 874–889.
[46] T. Chen, L. Zhao, X. Gao, L. Li, L. Qin, Modification of carbonation-cured cement mortar using biochar and its environmental evaluation, Cem. Concr. Compos. 134 (2022) 104764.
[47] M.G. Beltrán, A. Barbudo, F. Agrela, J.R. Jiménez, J. de Brito, Mechanical performance of bedding mortars made with olive biomass bottom ash, Constr. Build. Mater. 112 (2016) 699–707.
[48] M.E.G. Dobrovolski, G.S. Munhoz, E. Pereira, R.A. Medeiros-Junior, Effect of crystalline admixture and polypropylene microfiber on the internal sulfate attack in Portland cement composites due to pyrite oxidation, Constr. Build. Mater. 308 (2021) 125018.
[49] A. Akhtar, A.K. Sarmah, Novel biochar-concrete composites: manufacturing, characterization and evaluation of the mechanical properties, Sci. Total Environ. 616-617 (2018) 408–416.
[50] M.I. Khan, M.A. Abdy Sayyed, M.M.A. Ali, Examination of cement concrete containing micro silica and sugarcane bagasse ash subjected to sulphate and chloride attack, Mater. Today.: Proc. 39 (2021) 558–562.
[51] H.K. Venkatanarayanan, P.R. Rangaraju, Evaluation of sulfate resistance of portland cement mortars containing low-carbon rice husk ash, J. Mater. Civ. Eng. 26 (4) (2014) 582–592.
[52] P. Zhan, J. Wang, H. Zhao, W. Li, S.P. Shah, J. Xu, Impact of synthetic C-S-H seeds on early hydration and pore structure evolution of cement pastes: a study by 1H low-field NMR and path analysis, Cem. Concr. Res. 175 (2024) 107376.
[53] Z. Wang, H. Jiang, Y. Fu, Z. Ma, X. Wang, Calcined alunite-modified alkali-sulphate-activated slag as a novel binder for high-performance cemented paste backfill, J. Build. Eng. 91 (2024) 109687.
[54] S. Boudache, A. Loukili, L. Izoret, E. Rozière, Investigating the role played by portlandite and C-A-S-H in the degradation response of pozzolanic and slag cements to external sulphate attack, J. Build. Eng. 67 (2023) 106053.
[55] F.S. Hashem, T.A. Razek, H.A. Mashout, F. A.Selim, Fabrication of slag/CKD one-mix geopolymer cement reinforced by low-cost nano-particles, mechanical behavior and durability performance, Sci. Rep. 14 (1) (2024) 2549.
[56] C. Qiao, P. Suraneni, J. Weiss, Damage in cement pastes exposed to NaCl solutions, Constr. Build. Mater. 171 (2018) 120–127.
[57] D. Sugiyama, Chemical alteration of calcium silicate hydrate (C–S–H) in sodium chloride solution, Cem. Concr. Res. 38 (11) (2008) 1270–1275.
[58] S.S. Senadheera, S. Gupta, H.W. Kua, D. Hou, S. Kim, D.C.W. Tsang, Y.S. Ok, Application of biochar in concrete – a review, Cem. Concr. Compos. 143 (2023) 105204.
[59] M.S. Amin, F.A. Selim, M. Ramadan, A. Mohsen, A.M. Abu-Dief, H.A. Ahmed, F. S. Hashem, Evaluation of mechanical performance, corrosion behavior, texture characterization and aggressive attack of OPC-FMK blended cement pastes modified with micro Titania, Constr. Build. Mater. 416 (2024) 135261.